Int. J. Electrochem. Sci., 16 **(2021)** Article ID: 210812, doi: 10.20964/2021.08.14

International Journal of
ELECTROCHEMICAL
SCIENCE
www.electrochemsci.org

Monitoring Glucose in Fermented Beer by an Electrochemical Sensor Based on Graphene Oxide Decorated by Silver Nanoparticles

Yin Feng[*], *Yan Liu*[*], *Bo Feng*, *Haiyan Chen*, *Lixin You*[1], *Huaiquan Pei*[1]

School of Life Sciences, Changchun SCI-TECH University, Changchun 130000, China
[*]E-mail: fengyin1123@sina.com , ly78210310@sina.com

Received: 7 April 2021/ *Accepted:* 26 May 2021 / *Published:* 30 June 2021

The aim of this research was to create a non-enzymatic sensor for electrochemical glucose monitoring during the glycolytic process using functionalized graphene oxide decorated with silver nanoparticles modified glassy carbon electrode (Ag NPs/f-GOx/GCE). The Hummers method was used to synthesize GOx, which was then functionalized before being decorated with Ag NPs. The prepared GOx nanosheets oriented at different angles, rippled, and entangled with each other, and the Ag NPs in fcc structure were strongly and irregularly immobilized on GOx nanosheets in spherical form, according to morphological and structural studies using SEM and XRD analyses. The electrochemical studies using CV and amperometry techniques revealed that Ag NPs/f-GOx/GCE has a high stability and sensitivity, with sensitivity, detection limit, and linear range of 2.94 µA/µM, 0.001 µM, and 0 to 28 µM, respectively. When comparing the glucose sensing properties of Ag NPs/f-GOx/GCE to those of other non-enzymatic glucose sensors, it was discovered that Ag NPs/f-GOx/GCE had the lowest detection limit and the highest sensitivity values due to the synergetic effect of Ag NPs and f-GOx on Ag NPs/f-GOx/GCE, which have great structural characteristics and significant amounts of electroactive sites. The analysis of interference effect in the presence of potential interfering species during the glycolytic process revealed the prepared glucose sensor's high sensitivity and selectivity. The practical application of the proposed sensor to determine glucose in a fermented beer sample revealed that Ag NPs/f-GOx/GCE has the potential to be a reliable glucose determination sensor during glucose fermentation.

Keywords: Glucose; Amperometry; fermentation**;** Graphene oxide; Silver nanoparticles

1. INTRODUCTION

Glucose sensors have become increasingly popular and critical devices for healthcare and clinical diagnosis in recent years due to growing demand[1, 2]. Moreover, these sensors have been increasingly used as analytical tools in the chemical, fermentation engineering, food and drink industries [3]. Glucose molecules show a significant role in fermentation reactions and heterotrophic

metabolism for growth and synthesis of bacteria, containing oxidation of glucose by aerobic organisms in fundamental biochemical pathways which are related to oxidative components such as phosphorylation, glycolytic, citric acid, and tricarboxylic acid [4, 5]. Fermentation begins with glycolysis which breaks down glucose molecules into two pyruvate molecules and produces two adenosine triphosphate and two nicotinamide adenine dinucleotide [6]. As a result, numerous studies have been conducted to determine glucose using methods such as iodometry, polarimetry, optical coherence tomography, colorimetry, photoacoustic, chromatography, near-infrared (NIR) spectroscopy, Raman spectroscopy, diffuse reflection spectroscopy, fluorescence spectroscopy, thermal emission spectroscopy, electrochemical and photoelectrochemical methods [7-9]. Among them, the enzymatic and non-enzymatic electrochemical glucose sensors have been shown to have significant efficiency in determination of glucose in blood and food samples [10].

For monitoring of glucose in fermented food or during the glycolytic process, glucose biosensors have often relied on immobilization of glucose oxidase enzyme as the most popular bio-recognition element on different modified electrodes to convert bio-recognition events into a measurable signal. Studies are evidence of high selectivity and sensitivity of enzymatic glucose biosensors. However, the enzyme-based biosensors have not been shown enough stability in a wide range of pH and temperature, and side products and harmful chemicals in the complex fermentation process [11, 12].

Further electrochemical studies on non-enzymatic glucose sensors such as Pt, Au and transitional metals electrodes have represented the more stable and wide linear range sensors [13-15]. Furthermore, the development of nanostructured sensors provides a high effective surface area and a fast electron transfer rate, which improves sensor selectivity [16-19]. Studies have been revealed that the GOx can be a low cost and efficient material to improve the sensitivity of electrochemical sensors [20, 21]. In addition, functionalization of GOx and its decoration via metallic nanoparticles enhance the surface loading of glucose molecules and decreases the detection limit of non-enzymatic glucose sensors. Thus, this study was conducted on the synthesis of Ag NPs/f-GOx/GCE as a non-enzymatic electrochemical sensor for monitoring of glucose during the glycolytic process.

2. MATERIALS and METHOD

GOx was synthesized using the Hummers method [22]. 10 g of graphite powder (99%, Hebei Xingshi Import And Export Co., Ltd., China) was added to 5g $KMnO_4$ (≥99.0%, Sigma-Aldrich) and 5g K_2FeO_4 (>99%, Hongkong Xinrunde Chemical Co., Ltd., China) as the oxidants, then mixed with 0.05 g of boric acid (>99%) as a stabilizer. The mixture was ultrasonically dispersed in 0.1L of sulfuric acid (98%) at 6 °C for 90 minutes. After that, 300 mL of deionized (DI) water was gradually added to the mixture under stirring at 80°C for 30 min. Subsequently, 15 mL H_2O_2 (33%) was added to the resulting brown suspension. The mixture was centrifuged at 5000 rpm for 40 minutes. The obtained GOx was repeatedly washed with 1M HCl (33%), DI water and ethanol; respectively. 1 mg (3-mercaptopropyl) trimethoxysilane (MPTS, 95%, Sigma-Aldrich) was ultrasonically added to a GOx suspension at 70 °C for 120 minutes to form the mercapto groups on the GOxnanosheets. For

elimination of unreacted MPTS, the functionalized GOx was repeatedly washed with ethanol and dried in an oven at 80 °C.

In order to synthesize the Ag NPs, 0.02 g $AgNO_3$ (≥99.0%, Sigma-Aldrich) and 5 mL trisodium citrate (1 wt%, Sigma-Aldrich) were dissolved in 0.20 L DI water under stirring at 100°C for 30 minutes to obtained the light yellow solution. Afterward, for obtain the yellow green suspension of Ag NPs, the stirring of solution was continued for 60 minutes at 10°C. In order to preparation the Ag NPs/GOx, 50 mg of the functionalized GOx was ultrasonically dispersed in 50 mL DI water for 60 minutes. Subsequently, 10 mL of prepared Ag NPs suspension were ultrasonically added for 20 minutes. The obtained Ag NPs/GOx mixture was aged for 7 hours at ambient temperature and then was centrifuged and rinsed with DI water. Finally, the resulted product was dried in oven at 80 °C.

The morphology and crystal structure of p Ag NPs/f-GOx were studied by scanning electron microscopy (SEM,JEOL, JFC1600,Japan) and x-ray diffraction (XRD, Shimadzu 6000, operated at 40 kV and 30 mA, wavelength radiation of CuKα (λ=1.5418 Å), Japan). Amperometry and cycle voltammetry (CV) analyses were performed for electrochemical studies using Autolab Potentiostat (Metrohm Autolab B. V., Netherlands) in a three-electrode electrochemical cell which contained the Ag/AgCl electrode as reference electrode, Pt plate as counter electrode and modified GCE as working electrode. 0.1 M NaOH (99%, Vg International Trade (Shandong) Co., Ltd., China) solution was used as an electrolyte for electrochemical measurements because it facilitated the ionic conductivity and helped glucose molecules to move swiftly toward the electrode.

Beer and honey samples were provided by Jiangsu supermarket for the preparation of real samples according to [23]. 0.3 L of honey was dissolved in 0.8 L of deionized water and heated for 20 minutes at 80 °C. After cooling the solution, potassium metabisulfite (99%, Hebei Mojin Biotechnology Co., Ltd., China) was added to pasteurize the honey solution and left for 12 hours. Then, it was added directly to the 1L beer sample. 10g/L Saccharomyces cerevisiae yeast (99%, Henan JDZ Bio-Engineering Co., Ltd., China) solution was added to the resulting solution. It was taken at room temperature in unopened packages for 2, 4 and 8 days in a platform shaker (CAPPRondo, Germany) to evaluate potential variation in carbohydrate composition and glycolytic process. Afterward, the samples were centrifuged at 1000 rpm for 15 minutes. The resulting supernatants were filtered and used for preparation of 0.1M NaOH. The samples were stored in a refrigerator at 4°C for electrochemical measurements. The samples were analyzed using both the glucosemeter (Accuchek; Roche Diagnostic Corporation, Indianapolis, IN) and the amperometry technique, which was performed on Ag NPs/f-GOx/GCE in prepared samples and successive injections of glucose in 0.1 M NaOH solution at 0.40 V.

3. RESULTS AND DISCUSSION

3.1 Morphological and structural studies

The morphology of prepared functionalized GOx and Ag NPs/GOx are shown in SEM images from Figure 1a and 1b, respectively. As observed, the GOx are assembled into wrinkling structures which are similar to crumpled silk veils. The nanosheets were oriented at different angles, rippled, and

became entangled with one another. The SEM image of Ag NPs/GOx shows the Ag NPs are immobilized on GOx nanosheets in a spherical shape with an average diameter of 70 nm. The GOx nanosheets are strongly and irregularly decorated with Ag NPs because of repulsive interactions between the irregular agglomerated nanocrystals on the GOx surface.

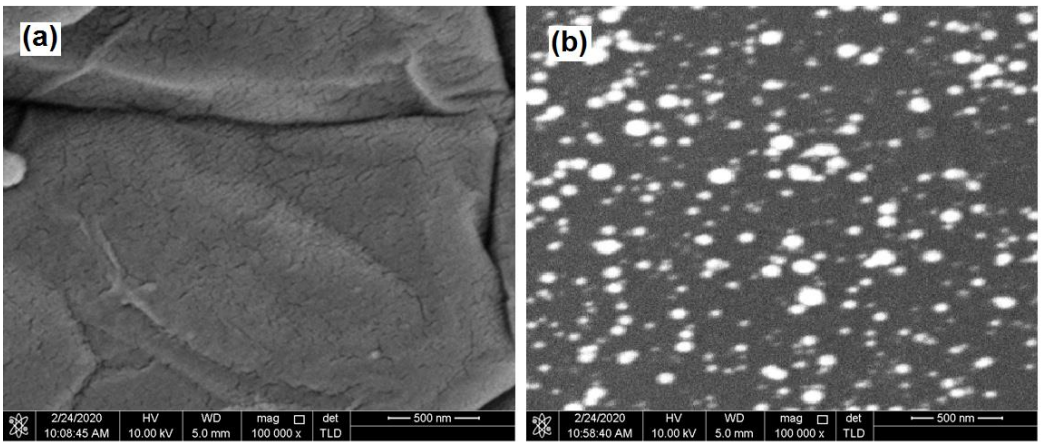

Figure 1. FESEM image of (a) prepared functionalized GOx and (b) Ag NPs/GOx.

Figure 2 shows the XRD pattern of prepared functionalized GOx and Ag NPs/GOx. As seen from the XRD pattern of functionalized GOx, there are two diffraction peaks at 2θ = 9.11° and 20.59° which representthe formation of (001) and (002) graphitic planes [24], respectively. XRD pattern of Ag NPs/GOx Figure 2b displays the additional peaks at 38.56°, 44.33°, 64.40° and 77.59° which corresponded to the formation the face-centered-cubic (fcc) structure of Ag NPs with (111), (200), (220) and (311) planes [25]. The results indicate that Ag NPs were successfully distributed on the GOx nanosheets.

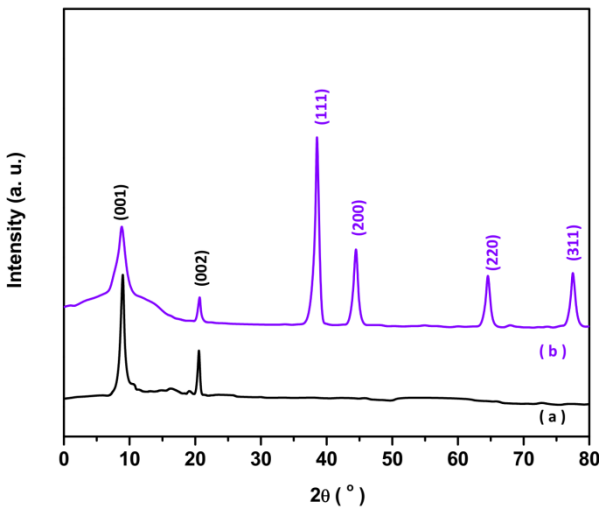

Figure 2. XRD patterns of (a) prepared functionalized GOx and (b) Ag NPs/GOx.

3.2 Electrochemical studies

The electrocatalytic properties of GCE, f-GOx/GCE and Ag NPs/f-GOx/GCE modified GCE were investigated in a 0.1 M NaOH solution at a scan rate of 50 mV/s. As seen from Figures 3a and 3b, no peak are observed for GCE, f-GOx/GCE. Figure 3c shows that the background current and area enclosed by the CV curve of f-GOx/GCE is more than GCE, which is related to large effective surface area and higher conductivity of f-GOx nanosheets that facilitate the electron transfer in the electrocatalytic process [26]. The modification of the GCE with Ag NPs decorated f-GOx results in sharp anodic peaks at 0.03, 0.25, and 0.44 V, corresponding to the electro-formation of Ag_2O, formation of Ag_2O, and oxidation of Ag_2O to AgO on the f-GOx surface[27], respectively. Moreover, two cathodic peaks at 0.34 and -0.01 V which are associated with the reduction of AgO to Ag_2O, and reduction of Ag_2O to Ag [28], respectively.

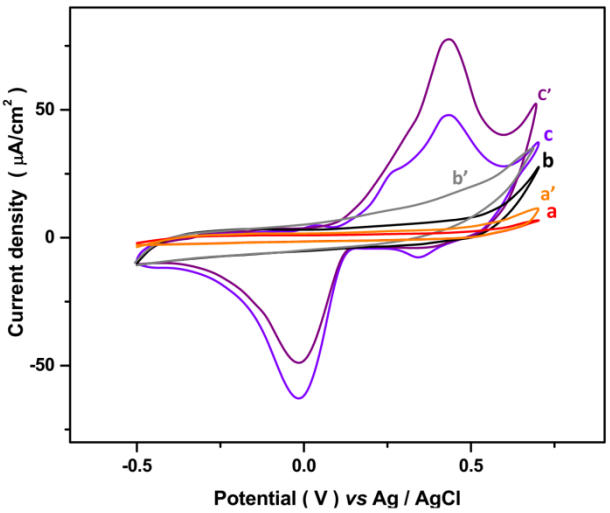

Figure 3. The CV curves of (a, a') GCE, (b, b') f-GOx/GCE and (c, c') Ag NPs/f-GOx/GCE modified GCE in 0.1 M NaOH solution at scan rate of 50 mV/s in 'absence and presence of 10 μM glucose.

CV curves in Figure 3a', 3b' and 3c' show the electrocatalyic responses of modified electrodes in 0.1 M NaOH solution containing 210 μM glucose at a scan rate of 50 mV/s. As seen in Figure 3c ', the CV curve of Ag NPs/f-GOx/GCE (Figure 3c ') shows a significant improvement in current density at 0.44 V in the presence of 10 M glucose compared to GCE (Figure 3a'), f-GOx/GCE (Figure 3b '), indicating a strong electroactive response of decorated Ag NPs on f-GOx to glucose determination. The synergetic effect of Ag NPs on f-GOx could accelerate the electron transfer between electro-active sites on electrode and electrolyte [29, 30]. The electrocatalytic response of the Ag NPs/f-GOx towards glucose is attributed to dehydrogenation and adsorption of the glucose molecules on the surface of the Ag NPs/f-GOx. Subsequently, the high density of electrochemically active sites of metal-OH on the electrode surface intermediates for the formation of gluconolactone [31]. Thus, the further electrochemical studies were conducted on Ag NPs/f-GOx/GCE. The following equations [32]can be

used to assign the electrocatalytic glucose oxidation mechanism to Ag oxidation and reduction reactions:

$$Ag + 2OH^- \rightarrow Ag(OH)_2 + 2e^- \quad (1)$$
$$Ag(OH)_2 + OH^- \rightarrow AgO(OH) + H_2O + e^- \quad (2)$$
$$AgO(OH) + Glucose \rightarrow Ag(OH)_2 + glucolactone \quad (3)$$

The obtained results are consistent with those obtained in nonenzymatic glucose sensors based on core-shell gold-nickel nanostructured and Au-Ag NPs modified GCE [33, 34].

Figure 4a shows the amprometric response of Ag NPs/f-GOx/GCE to successive injections of 1 µM glucose in 0.1 M NaOH solution at 0.40 V and a rotating speed of 1500 rpm. The fast response is observed for any injection of 1 µM glucose solution. The calibration plot in Figure 4b shows increase of the electrocatalytic current with increasing the glucose concentration in electrolyte. The calibration plot yielded the sensitivity, detection limit, and linear range of 2.94 µA/µM, 0.001 µM, and 0 to 28 µM, respectively.

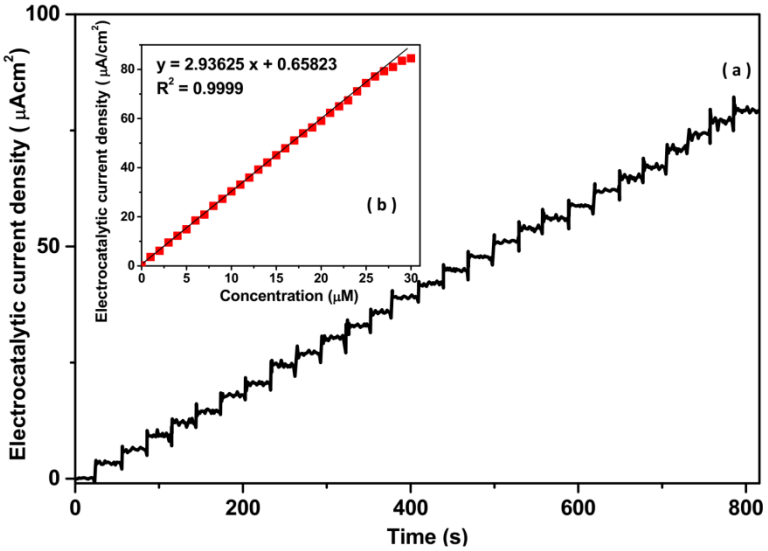

Figure 4. (a) Amprometric response of Ag NPs/f-GOx/GCE to successive injections of 1 µM glucose in 0.1 M NaOH solution at 0.40 V and rotating speed of 1500 rpm. (b) Calibration plot.

Table 1. Comparison between the obtained glucose sensing property of Ag NPs/f-GOx/GCE and other non-enzymatic reported glucose sensors based GOx, CNTs and Ag NPs.

Electrodes	**Method**	**limit of detection(µM)**	**Linear Range(µM)**	**Sensitivity (µA/µM)**	**Ref.**
Ag–polyaniline/rGOnanocomposites	Amperometry	0.79	0.14- 50	2.7664	[35]
Ag/CNTs	DPV	10.0	25 - 1000	0.014	[30]
Ag/Ag2O-rGO	Amperometry	60	200–8000	0.032	[36]

Ag-NW/RGO 3D nanostructure	Amperometry	0.48	1000 - 10000	0.877	[37]
RGO– Polyamidoamine –Ag nanocomposite	CV	4.5	32 - 189	0.07572	[38]
Ag@TiO2@ Metal-Organic Framework	Amperometry	0.99	48 - 1000	0.788	[39]
nanoporous Ag flowers/Ni	Amperometry	0.1	0.1 - 1000	1.549	[40]
Nickel Oxides Nanoparticle/ Graphene Composite	DPV	0.42	1–1800	0.1075	[41]
Au-rGO-SWCNT	LSV	0.0022	0–80000	-	[42]
Au/rGtO	Amperometry	63.0	0–10000	0.0398	[43]
Ag NPs/f-GOx/GCE	Amperometry	0.001	0-28	2.93625	This work

Table 1 demonstrates the comparison between obtained glucose sensing properties of Ag NPs/f-GOx/GCE and other reported glucose sensors which display the lowest detection limit and highest sensitivity values of Ag NPs/f-GOx/GCE than other non-enzymatic reported glucose sensors based onGOx, CNTs and Ag NPs due to synergetic effect of Ag NPs and f-GOx which provide the great structural characteristic and large amounts of elecroactive sites on Ag NPs/f-GOx/GCE. The good electrical conductivity and fast electron transfer of Ag NPs could be responsible for enhancement of sensitivity. The functionalized GOx can be an efficient way to improve the conductivity of GOx[20]. Moreover, after functionalization, the decorated electrode exhibits new desirable properties due to overcome the disadvantages of intrinsic GOx [20]. Therefore, the large surface area of Ag NPs/f-GOx/GCE can enhance the surface loading of glucose molecules and decrease the detection limit value.

The stability of amprometric response of Ag NPs/f-GOx/GCE was studied with injections of 10 μM glucose in 0.1 M NaOH solution at 0.40 V and a rotating speed of 1500 rpm. Figure 5 shows the decrease of 4% after 10 minutes, indicating the high stability of the proposed sensor for determination of glucose. The interference effect of glucose sensor was investigated in the presence of the possible interfering species during the glycolytic process according to studies [44, 45]. Concentrations of species were chosen based on relative concentrations in the glycolytic process. Table 2 represents the amperometric response of Ag NPs/f-GOx/GCE to injection of the interfering species and glucose in 0.1 M NaOH solution at 0.40 V. It is discovered that injection of glucose solution produces a significant response. While, it hasn't observed any significant response to injection of other interfering substrates at 0.40 V, which indicated the species in Table 2 don't show interfere with detection of glucose by Ag NPs/f-GOx/GCE during the glycolytic process. Therefore, it reveals the great sensitivity and selectivity of prepared glucose sensor.

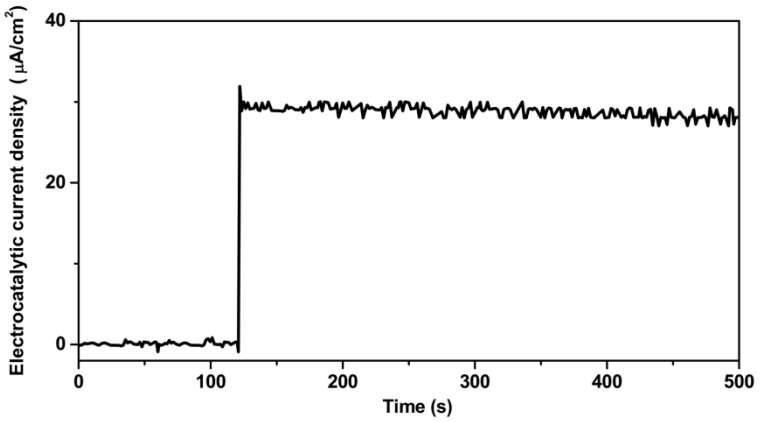

Figure 5. The amprometric response of Ag NPs/f-GOx/GCE to injections of 10 μM glucose in 0.1 M NaOH solution at 0.40 V and rotating speed of 1500 rpm

Table 2. Electrocatalytic responses of Ag NPs/f-GOx/GCE to injection of the interfering species and glucose in 0.1 M NaOH solution at 0.40 V

Substance	**Added (g/l)**	**Electrocatalytic current response (μA)**	**RSD (%)**
Glucose	10	29.01	±0.75
$(NH_4)_2SO_4$	6	1.01	±0.02
K_2HPO_4	4	0.99	±0.08
KH_2PO_4	5	0.90	±0.09
$MgSO_4{\cdot}7H_2O$	35	1.82	±0.05
Fructose	56	1.53	±0.07
Sucrose	3	0.58	±0.04
Propionic acid	1	0.22	±0.04
Citric acid	10	0.99	±0.02
Malic acid	5	0.72	±0.03

A glucosemeter was used to assess the practical applicability of the proposed sensor for determining glucose in prepared fermented beer samples after 2, 4, and 8 days. Then, the amprometric response of Ag NPs/f-GOx/GCE was recorded for fermented beer samples to successive injections of glucose in 0.1 M NaOH solution at 0.40 V. The calibration plots of proposed sensor are shown in Figure 6. Table 3 shows that the obtained glucose concentrations of three samples are consistent with the obtained values by the glucosemeter. These results are in agreement with the report by Samphao et al. [23] for determination of glucose content in fermented beer samples. Therefore, the Ag NPs/f-GOx/GCE can be reliable in practical potential for glucose determination during the glycolytic process.

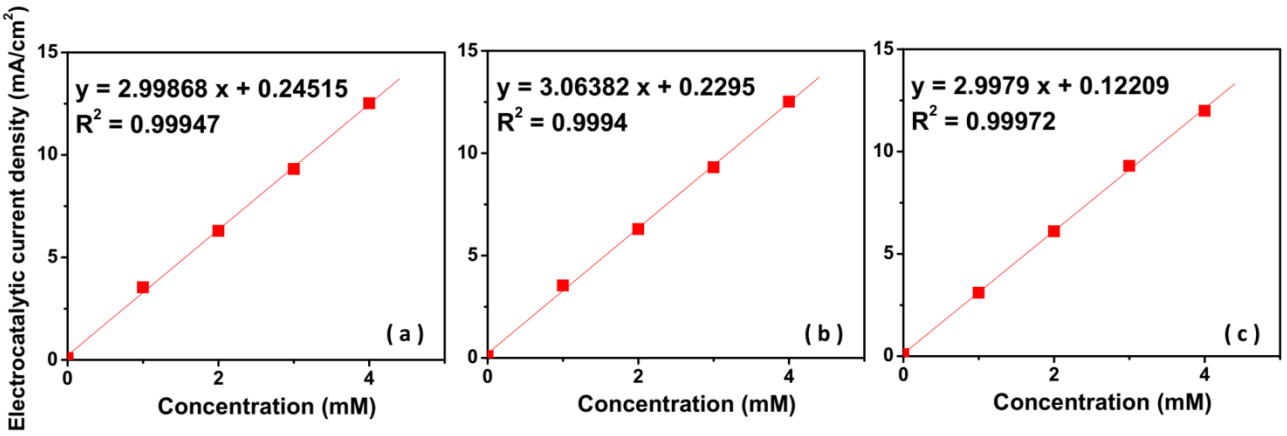

Figure 6. Calibration plots of amprometric response of Ag NPs/f-GOx/GCE at 0.40 V and rotating speed of 1500 rpm to successive injections of 1 mM glucose in 0.1 M NaOH solution prepared fermented beer samples after (a) 2, (b) 4, and (c) 8 days.

Table 3. Determination of glucose from fermented beer samples using Ag NPs/f-GOx/GCE and glucose meter

fermented beer samples	**Obtained value by Ag NPs/f-GOx/GCE (µM)**	**Obtained value byglucosemeter (µM)**
2 days	81 ± 1.07	83
4 days	75 ± 0.91	75
8 days	40 ± 0.45	43

4. CONCLUSION

This research was done to create Ag NPs/f-GOx/GCE as a non-enzymatic sensor for electrochemical glucose determination during the glycolytic process. The Hummers method was applied to synthesis of GOx nanosheets which were then chemically functionalized in an acidic solution before being decorated with Ag NPs. The Ag NPs in fcc structure were strongly and irregularly immobilized on GOx nanosheets in spherical form, according to morphological and structural studies. The electrochemical studies displayed the high stability and high sensitivity of Ag NPs/f-GOx/GCE. The sensitivity, detection limit, and linear range were calculated to be 2.94 µA/µM, 0.001 µM, and 0 to 28 µM, respectively. The analysis of interference effect in the presence of potential interfering species during the glucose glycolytic process revealed the prepared glucose sensor's high sensitivity and selectivity. The practical application of the proposed sensor to determine glucose in a fermented beer sample revealed that Ag NPs/f-GOx/GCE has the potential to be a reliable glucose determination sensor during the glycolytic process.

ACKNOWLEDGEMENT
The work was funded by the “Thirteen-five" science and technology project (JJKH20201292JY) of The Education Department of Jilin Province of China.

References

1. M. Goodarzi, S. Sharma, H. Ramon and W. Saeys, *TrAC Trends in Analytical Chemistry*, 67 (2015) 147.
2. H. Karimi-Maleh, Y. Orooji, A. Ayati, S. Qanbari, B. Tanhaei, F. Karimi, M. Alizadeh, J. Rouhi, L. Fu and M. Sillanpää, *Journal of Molecular Liquids*, 329 (2021) 115062.
3. R. Zhao, Y. Wang, Y. Hasebe, Z. Zhang and D. Tao, *International Journal of Electrochemical Science*, 15 (2020) 1595.
4. D. Uner-Bahar and I. Isildak, *International Journal of Electrochemical Science*, 15 (2020) 12724.
5. J. Rouhi, S. Kakooei, M.C. Ismail, R. Karimzadeh and M.R. Mahmood, *International Journal of Electrochemical Science*, 12 (2017) 9933.
6. J.D. Rabinowitz and S. Enerbäck, *Nature Metabolism*, 2 (2020) 566.
7. X. Zhang and Q. Wang, *International Journal of Electrochemical Science*, 16 (2021) 151061.
8. Q. Yuan, Z. Zhang and L. Li, *International Journal of Electrochemical Science*, 15 (2020) 5245.
9. H. Karimi-Maleh, Y. Orooji, F. Karimi, M. Alizadeh, M. Baghayeri, J. Rouhi, S. Tajik, H. Beitollahi, S. Agarwal and V.K. Gupta, *Biosensors and Bioelectronics*, (2021)
10. P. Liu, L. Yin and X. Qi, *International Journal of Electrochemical Science*, 15 (2020) 5821.
11. J.I. Reyes-De-Corcuera, H.E. Olstad and R. García-Torres, *Annual review of food science and technology*, 9 (2018) 293.
12. J. Rouhi, H.K. Malayeri, S. Kakooei, R. Karimzadeh, S. Alrokayan, H. Khan and M.R. Mahmood, *International Journal of Electrochemical Science*, 13 (2018) 9742.
13. J. Wang, H. Gao, F. Sun and C. Xu, *Sensors and Actuators B: Chemical*, 191 (2014) 612.
14. C. Li, H. Wang and Y. Yamauchi, *Chemistry–A European Journal*, 19 (2013) 2242.
15. H. Karimi-Maleh, M.L. Yola, N. Atar, Y. Orooji, F. Karimi, P.S. Kumar, J. Rouhi and M. Baghayeri, *Journal of colloid and interface science*, 592 (2021) 174.
16. H. Savaloni, E. Khani, R. Savari, F. Chahshouri and F. Placido, *Applied Physics A*, 127 (2021) 1.
17. Z. Savari, S. Soltanian, A. Noorbakhsh and A. Salimi, *Electrochemical Society Iran*, 9 (2013) 1.
18. F. Chahshouri, H. Savaloni, M. Khoramshahi and R. Savari, *3rd International Biennial Oil, Gas and Petrochemical Conference*, 1 (2020) 1.
19. H. Karimi-Maleh, S. Ranjbari, B. Tanhaei, A. Ayati, Y. Orooji, M. Alizadeh, F. Karimi, S. Salmanpour, J. Rouhi and M. Sillanpää, *Environmental Research*, 195 (2021) 110809.
20. D. Saini, *Nanotechnology Reviews*, 5 (2016) 393.
21. H. Karimi-Maleh, M. Alizadeh, Y. Orooji, F. Karimi, M. Baghayeri, J. Rouhi, S. Tajik, H. Beitollahi, S. Agarwal and V.K. Gupta, *Industrial & Engineering Chemistry Research*, 60 (2021) 816.
22. N. Zaaba, K. Foo, U. Hashim, S. Tan, W.-W. Liu and C. Voon, *Procedia engineering*, 184 (2017) 469.
23. A. Samphao, P. Butmee, P. Saejueng, C. Pukahuta, Ľ. Švorc and K. Kalcher, *Journal of Electroanalytical Chemistry*, 816 (2018) 179.
24. J. Jagiełło, A. Chlanda, M. Baran, M. Gwiazda and L. Lipińska, *Nanomaterials*, 10 (2020) 1846.
25. M.M.R. Mollick, B. Bhowmick, D. Maity, D. Mondal, M.K. Bain, K. Bankura, J. Sarkar, D. Rana, K. Acharya and D. Chattopadhyay, *International Journal of Green Nanotechnology*, 4 (2012) 230.
26. H. Gul, A.-u.-H.A. Shah, U. Krewer and S. Bilal, *Nanomaterials*, 10 (2020) 118.

27. A.A. Ensafi, N. Zandi-Atashbar, B. Rezaei, M. Ghiaci, M.E. Chermahini and P. Moshiri, *RSC advances*, 6 (2016) 60926.
28. H. Quan, S.-U. Park and J. Park, *Electrochimica Acta*, 55 (2010) 2232.
29. S.A. Shabbir, S. Tariq, M.G.B. Ashiq and W.A. Khan, *Bioscience reports*, 39 (2019) 1.
30. L. Chen, H. Xie and J. Li, *Journal of Solid State Electrochemistry*, 16 (2012) 3323.
31. G. Amala and S. Gowtham, *RSC advances*, 7 (2017) 36949.
32. T.V. Kumar and A.K. Sundramoorthy, *Journal of The Electrochemical Society*, 165 (2018) B3006.
33. X. Gao, X. Du, D. Liu, H. Gao, P. Wang and J. Yang, *Scientific Reports*, 10 (2020) 1365.
34. N.G. García-Morales, L.A. García-Cerda, B.A. Puente-Urbina, L.M. Blanco-Jerez, R. Antaño-López and F. Castañeda-Zaldivar, *Journal of Nanomaterials*, 2015 (2015) 1.
35. M.A. Deshmukh, B.-C. Kang and T.-J. Ha, *Journal of Materials Chemistry C*, 8 (2020) 5112.
36. L. Shahriary and A.A. Athawale, *Journal of Solid State Electrochemistry*, 19 (2015) 2255.
37. V.H. Luan, J.H. Han, H.W. Kang and W. Lee, *Results in Physics*, 15 (2019) 102761.
38. Z. Luo, L. Yuwen, Y. Han, J. Tian, X. Zhu, L. Weng and L. Wang, *Biosensors and Bioelectronics*, 36 (2012) 179.
39. D. Arif, Z. Hussain, M. Sohail, M.A. Liaqat, M.A. Khan and T. Noor, *Frontiers in Chemistry*, 8 (2020) 1.
40. J. Chen, C. Liu, Y.-T. Huang, H. Lee and S.-P. Feng, *Nanotechnology*, 29 (2018) 505501.
41. A.M. MAZLOUM, F. Farbod and L. Hosseinzadeh, *Journal of Nanostructures*, 6 (2016) 293.
42. R.A. Escalona-Villalpando, M.P. Gurrola, G. Trejo, M. Guerra-Balcázar, J. Ledesma-García and L.G. Arriaga, *Journal of Electroanalytical Chemistry*, 816 (2018) 92.
43. Y. Luo, F.-Y. Kong, C. Li, J.-J. Shi, W.-X. Lv and W. Wang, *Sensors and Actuators B: Chemical*, 234 (2016) 625.
44. C.C.A.d.A. Santos, W.F. Duarte, S.C. Carreiro and R.F. Schwan, *Journal of the Institute of Brewing*, 119 (2013) 280.
45. H. Akin, C. Brandam, X.-M. Meyer and P. Strehaiano, *Chemical Engineering and Processing: Process Intensification*, 47 (2008) 1986.